Eur. Phys. J. C 23, 301–310 (2002)
Digital Object Identifier (DOI) 10.1007/s100520100883

THE EUROPEAN PHYSICAL JOURNAL C

Perturbative and non-perturbative QCD corrections to wide-angle Compton scattering

H.W. Huang[1,a], P. Kroll[2], T. Morii[1]

[1] Faculty of Human Development, Kobe University, Nada, Kobe 657-8501, Japan
[2] Fachbereich Physik, Universität Wuppertal, 42097 Wuppertal, Germany

Received: 31 October 2001 / Revised version: 11 December 2001 /
Published online: 8 February 2002 –

Abstract. We investigate corrections to the handbag approach for wide-angle Compton scattering off protons at moderately large momentum transfer: the photon–parton subprocess is calculated to next-to-leading order in α_s and contributions from the generalized parton distribution E are taken into account. Photon and proton helicity flip amplitudes are non-zero due to these corrections, which leads to a wealth of polarization phenomena in Compton scattering. Thus, for instance, the incoming photon asymmetry or the transverse polarization of the proton is non-zero, although small.

1 Introduction

Probing the proton with high-energy photons provides information about its inner structure. The most famous process used for such investigations is deep inelastic lepton–proton scattering. From a dynamical point of view this process represents forward (virtual) Compton scattering and is described by the handbag diagram shown in Fig. 1. Recent theoretical developments revealed that the physics of the handbag diagram is also of importance for deeply virtual [1,2] and wide-angle [3,4] Compton scattering off protons. Both these processes refer to complementary kinematical situations. The region of deeply virtual scattering is characterized by small momentum transfer from the initial to the final proton and a large photon virtuality, while in the wide-angle region the situation is reversed. As has been argued in [3,4] the wide-angle Compton amplitudes approximately factorize into hard photon–parton subprocess amplitudes and proton matrix elements representing the soft emission and reabsorption of a parton by the proton. These matrix elements are moments of generalized parton distributions (GPDs) [1,5,6] and can be regarded as new form factors of the protons. The GPDs also encode the soft physics information required to describe deeply virtual Compton scattering. That the handbag diagram, i.e. elastic scattering of photons from quarks, controls Compton scattering has been conjectured by Bjorken and Paschos [7] and by Scott [8] a long time ago as we note in passing.

It is however to be emphasized that the handbag contribution to wide-angle Compton scattering formally represents only a power correction to the leading-twist perturbative contribution [9]. This contribution for which all partons the proton is composed of participate in the hard scattering, and not only a single one as in the handbag model, has been calculated several times [10] with partially contradicting results. According to the most recent study [11], it seems difficult to account for the wide-angle data on Compton scattering [12]. This result as well as similar observations made with the pion and the proton electromagnetic form factors [13,14] have lead to the assumption of a dominant handbag contribution for momentum transfers below about $100\,\mathrm{GeV}^2$. There is a third contribution to Compton scattering. It has the topology of the so-called cat's ears graphs where the hard subprocess involves two partons. It is reasonable to assume that the magnitude of this contribution is intermediate between the handbag and the perturbative one and that it can be neglected in the kinematical range of interest.

In this work we are going to investigate perturbative and non-perturbative QCD corrections to the handbag contribution for wide-angle Compton scattering. We calculate the next-to-leading order (NLO) corrections to the subprocess and, motivated by the surprising result for the Pauli form factor found at JLab [15], we study the bearing of the form factor R_T, neglected in [3,4], on the predictions. We begin with a sketch of the handbag approach and the calculation of the NLO corrections (Sect. 2). A brief discussion of the model used for the form factors, or the underlying GPDs, follows (Sect. 3). Section 4 is devoted to a comprehensive discussion of the predictions for a large set of observables and their comparison with the results presented in [4] and with those obtained with other theoretical concepts. This may facilitate the interpretation of future experimental data on wide-angle Compton scattering that might be obtained at Spring-8, JLab or at an

[a] Postdoctoral research fellow (No. P99221) of the Japan Society for the Promotion of Science (JSPS)

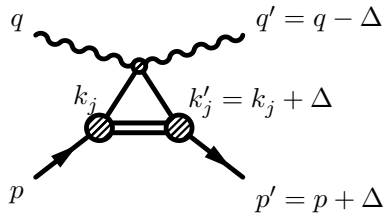

Fig. 1. The handbag diagram for Compton scattering off protons. The horizontal lines represent any number of spectator partons

ELFE-type accelerator. Finally we discuss the possibility of measuring the Compton form factors (Sect. 5) and close with a summary (Sect. 6).

2 The handbag contribution

Let us sketch the calculation of the handbag contribution to wide-angle Compton scattering; for details we refer to [4]. For Mandelstam variables, s, t and u, that are large on a hadronic scale, Λ^2, of the order of $1\,\mathrm{GeV}^2$, the Compton amplitudes are calculated from the handbag graph displayed in Fig. 1. Its contribution is defined through the assumption that the soft hadron wave functions occurring in the Fock decomposition of the proton, are dominated by parton virtualities in the range $|k_i^2| \lesssim \Lambda^2$ and by intrinsic transverse parton momenta $\boldsymbol{k}_{\perp i}$ that satisfy $\boldsymbol{k}_{\perp i}^2/x_i \lesssim \Lambda^2$. The intrinsic transverse momentum of a parton is defined in a frame where its parent's hadron transverse momentum is zero; $x_i = k_i^+/p^+$ is the usual light-cone momentum fraction. It is of advantage to choose a symmetric frame of reference where the plus and minus light-cone components of the momentum transfer, Δ, are zero (for the definition of the kinematics see Fig. 1). This implies $t = -\boldsymbol{\Delta}_\perp^2$ as well as a vanishing skewedness parameter, $\xi = (p - p')^+/(p + p')^+$. One can then show that the photon–parton scattering is hard and the momenta k_j, k'_j of the active partons, i.e. those to which the photons couple (see Fig. 1), are approximately on-shell, collinear with their parent hadrons and with momentum fractions $x_j = x'_j = 1$. This leads to an approximate equality of the Mandelstam variables in the photon–parton subprocess and in the overall photon–proton reaction up to corrections of order Λ^2/t.

In view of this the helicity amplitudes $\mathcal{M}_{\mu'\nu',\mu\nu}$ of wide-angle Compton scattering in the symmetric frame are given by

$$\begin{aligned}
&\mathcal{M}_{\mu'+,\mu+}(s,t) \qquad (1)\\
&\quad = 2\pi\alpha_{\rm em}\Big[\mathcal{H}_{\mu'+,\mu+}(s,t)(R_V(t)+R_A(t))\\
&\qquad +\mathcal{H}_{\mu'-,\mu-}(s,t)(R_V(t)-R_A(t))\Big],\\
&\mathcal{M}_{\mu'-,\mu+}(s,t)\\
&\quad = -\pi\alpha_{\rm em}\frac{\sqrt{-t}}{m}\left[\mathcal{H}_{\mu'+,\mu+}(s,t)+\mathcal{H}_{\mu'-,\mu-}(s,t)\right]R_T(t).
\end{aligned}$$

Here, μ (ν) and μ' (ν') denote the light-cone helicities [16,17] of the incoming and outgoing photon (proton), respectively. m is the proton mass. For the sake of legibility explicit helicities are labeled only by their signs. We emphasize that the proton helicity flip amplitudes have been neglected in [3,4]. Below we will discuss under which circumstances this is reasonable and when not. It is also important to realize that the amplitudes (1) are subject to uncontrolled corrections of order Λ^2/t arising from the approximations necessary to achieve the factorization of the handbag contribution as has been shown in [4].

The soft proton matrix elements, R_i ($i = V, A, T$), appearing in (1) represent new types of proton form factors. They are defined as $1/x$-moments of GPDs at zero skewedness. For active quarks of flavor a (u, d,...) they read

$$\begin{aligned}
R_V^a(t) &= \int_{-1}^{1}\frac{\mathrm{d}\bar{x}}{\bar{x}}H^a(\bar{x},0;t),\\
R_A^a(t) &= \int_{-1}^{1}\frac{\mathrm{d}\bar{x}}{\bar{x}}\mathrm{sign}(\bar{x})\widetilde{H}^a(\bar{x},0;t),\\
R_T^a(t) &= \int_{-1}^{1}\frac{\mathrm{d}\bar{x}}{\bar{x}}E^a(\bar{x},0;t), \qquad (2)
\end{aligned}$$

where $\bar{x} = (k_j + k'_j)^+/(p + p')^+$. The full form factors in (1), specific to Compton scattering, are given by

$$R_i(t) = \sum_a e_a^2 R_i^a(t), \qquad (3)$$

e_a being the charge of quark a in units of the positron charge. In principle there is a fourth form factor, related to the GPD $\widetilde{E}^a$, but it does not contribute to the Compton amplitudes in the symmetric frame. The form factors R_i^a also appear in wide-angle photo- and electroproduction of mesons [18].

Last but not least, the $\mathcal{H}_{\mu'\lambda',\mu\lambda}$ in (1) denote the $\gamma q \to \gamma q$ subprocess amplitudes where the helicities λ and λ' refer to the quarks now. To leading order (LO) these amplitudes are to be calculated from the Feynman graphs shown in Fig. 2a. One finds

$$\mathcal{H}^{\rm LO}_{++,++} = 2\sqrt{\frac{s}{-u}}, \quad \mathcal{H}^{\rm LO}_{-+,-+} = 2\sqrt{\frac{-u}{s}}, \quad \mathcal{H}^{\rm LO}_{-+,++} = 0. \qquad (4)$$

Since the quarks are taken as massless there is no quark helicity flip, $\mathcal{H}_{\mu'\lambda,\mu-\lambda} = 0$ to any order of $\alpha_{\rm s}$. Other helicity amplitudes are obtained from those given in (4) by parity and time reversal invariance:

$$\mathcal{H}_{-\mu'-\lambda',-\mu-\lambda} = \mathcal{H}_{\mu\lambda,\mu'\lambda'} = (-1)^{\mu-\lambda-\mu'+\lambda'}\mathcal{H}_{\mu'\lambda',\mu\lambda}. \qquad (5)$$

Analogous relations hold for the $\mathcal{M}_{\mu'\nu',\mu\nu}$.

The NLO corrections to the $\gamma q \to \gamma q$ are to be calculated from the Feynman graphs b–e depicted in Fig. 2. We work in Feynman gauge and use dimensional regularization ($n = 4 + \epsilon$). As expected for the process at hand, the ultraviolet divergencies of the individual graphs cancel in the sum; the NLO amplitudes are ultraviolet safe. On

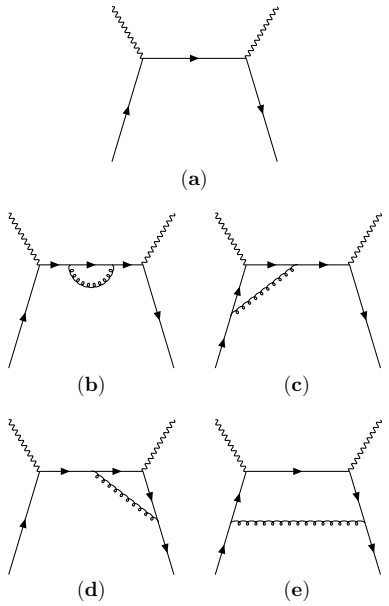

Fig. 2a–e. Feynman graphs for Compton scattering off on-shell quarks. **a** is the LO graph, the others represent the NLO QCD corrections. Graphs with self-energy corrections to external fermions and those with interchanged interaction points of the photons are not shown

the other hand, those photon helicity non-flip amplitudes which are non-zero at LO, are infrared (IR) divergent. They can be decomposed into an infrared divergent part $\propto \mathcal{H}^{\rm LO}$ and an infrared safe one, $\mathcal{H}^{\rm NLO}$,

$$\mathcal{H}^{\rm IR}_{\mu+,\mu+} = \frac{\alpha_{\rm s}}{4\pi} C_F C_{\rm IR}(\mu_F) \mathcal{H}^{\rm LO}_{\mu+,\mu+} + \mathcal{H}^{\rm NLO}_{\mu+,\mu+}, \qquad (6)$$

where $C_{\rm IR}$ embodies the IR singularities. C_F $(= 4/3)$ is a colour factor and μ_F is a factorization scale of order Λ. As usual, we interpret the infrared divergent pieces as non-perturbative physics and absorb them into the soft form factors. Thus, we write for any of the products of hard scattering amplitudes and form factors appearing in (1)

$$\begin{aligned}
&\mathcal{H}_{\mu+,\mu+}(s,t) R_i(t) \\
&= \left[\mathcal{H}^{\rm LO}_{\mu+,\mu+} \left(1 + \frac{\alpha_{\rm s}}{4\pi} C_F C_{\rm IR}(\mu_F)\right) + \mathcal{H}^{\rm NLO}_{\mu+,\mu+}\right] R_i(t) \\
&= \left[\mathcal{H}^{\rm LO}_{\mu+,\mu+} + \mathcal{H}^{\rm NLO}_{\mu+,\mu+}\right] R_i(t,\mu_F) + \mathcal{O}(\alpha_{\rm s}^2). \qquad (7)
\end{aligned}$$

The next issue we are concerned with is the exact definition of $C_{\rm IR}$. The infrared divergencies in (6) have the form

$$-\left(\frac{-t}{4\pi\mu_F^2}\right)^{\epsilon/2} \Gamma(1-\epsilon/2)(8/\epsilon^2 - 6/\epsilon). \qquad (8)$$

The $1/\epsilon^2$ term appears as a consequence of overlapping soft and collinear divergencies. The accompanying double logs become large at large $-t$ and have to be resummed together with corresponding higher order terms $[\alpha_{\rm s} \ln^2(-t/\mu_F^2)]^n$ in a Sudakov factor [19]. The same problems occur in the Feynman contribution to the electromagnetic form factor of the proton which is the analogue of the handbag contribution to Compton scattering. To NLO the $\gamma^* \to q\bar{q}$ vertex appearing in that calculation provides infrared singularities identically to (8) which have to be absorbed into the soft hadronic matrix element, too. It is, of course, natural to use the same scheme for the regularization of the IR divergencies for both the Feynman and the handbag contribution. Since customarily the Sudakov factor is considered as part of the electromagnetic form factor [19,20], i.e. the latter already includes resummed double logs, we are forced to identify $C_{\rm IR}$ with the full expression (8) in order to match with standard phenomenology and, in particular, with the model we employ in our numerical studies of Compton scattering. We remark in passing that the $\gamma^* \to q\bar{q}$ vertex also occurs in $e^+e^- \to q\bar{q}$. In this case the infrared singularities (8) are compensated by real gluon emission. The infrared divergencies generated by the NLO QED corrections to Compton scattering off electrons cancel against those of double Compton scattering, $\gamma e \to \gamma\gamma e$ [21]. In deeply virtual Compton scattering only a single IR pole appears [22] but it can be shown that in the limit $x_j \to 1$ an additional singularity emerges [23].

After removal of the IR divergencies the NLO amplitudes read

$$\begin{aligned}
\mathcal{H}^{\rm NLO}_{++,++} &= \frac{\alpha_{\rm s}}{2\pi} C_F \left\{ \frac{\pi^2}{3} - 7 + \frac{2t-s}{s} \ln\frac{t}{u} \right. \\
&\quad \left. + \ln^2\frac{-t}{s} + \frac{t^2}{s^2}\left(\ln^2\frac{t}{u} + \pi^2\right) - 2{\rm i}\pi \ln\frac{-t}{s} \right\} \sqrt{\frac{s}{-u}}, \\
\mathcal{H}^{\rm NLO}_{-+,-+} &= \frac{\alpha_{\rm s}}{2\pi} C_F \left\{ \frac{4}{3}\pi^2 - 7 + \frac{2t-u}{u} \ln\frac{-t}{s} + \ln^2\frac{t}{u} \right. \\
&\quad \left. + \frac{t^2}{u^2} \ln^2\frac{-t}{s} - 2{\rm i}\pi \left(\frac{2t-u}{2u} + \frac{t^2}{u^2}\ln\frac{-t}{s}\right) \right\} \sqrt{\frac{-u}{s}}, \\
\mathcal{H}^{\rm NLO}_{-+,++} &= -\frac{\alpha_{\rm s}}{2\pi} C_F \left\{ \sqrt{\frac{s}{-u}} + \sqrt{\frac{-u}{s}} \right\}. \qquad (9)
\end{aligned}$$

Since in wide-angle Compton scattering $-t$ and $-u$ are of order s there are no large logs in the NLO amplitudes. We also see that the NLO amplitudes possess both non-zero imaginary parts and non-zero photon helicity flips.

At the one-loop level, there is a complication which we have to discuss next, namely gluons have to be considered as active partons as well. The treatment of the gluonic contributions to wide-angle Compton scattering is analogous to that one utilized in wide-angle photo- and electroproduction of vector mesons [18]. The gluonic contributions factorize into the parton subprocess $\gamma g \to \gamma g$ and gluonic form factors. In contrast to the case of quarks, the partonic amplitudes now allow parton, i.e. gluon helicity flips to occur.

For gluon helicity non-flip the gluonic contributions have a representation analogous to (1). The corresponding form factors read

$$R_V^g(t) = \sum_a e_a^2 \int_0^1 \frac{{\rm d}\bar{x}}{\bar{x}^2} H^g(\bar{x},0;t), \qquad (10)$$

and analogously for the other ones. The range of integration is restricted to the interval $[0,1]$ since gluons and antigluons are the same particles. The additional factor

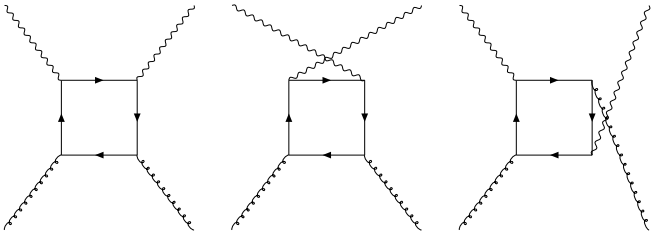

Fig. 3a–c. Sample Feynman graphs for photon–gluon scattering

$1/\bar{x}$ is conventional; it appears as a consequence of the definition of the gluon GPDs [1,5,6] which implies the forward limits

$$\bar{x}g(\bar{x}) = H^g(\bar{x},0;0), \quad \bar{x}\Delta g(\bar{x}) = \widetilde{H}^g(\bar{x},0;0). \tag{11}$$

With regard to this definition we still call (10) a $1/\bar{x}$-moment. The sum in (10) runs over the flavors u, d, s which suffices for the range of energy we are interested in. For gluon helicity flip we do not present details here because these contributions are neglected in our numerical studies as those proportional to the form factors R_A^g and R_T^g. This is justified since, as we will argue in Sect. 3, the gluon form factors are expected to be smaller than the corresponding quark ones at large $-t$ and since the gluonic contributions only appear to order α_s. Hence, we only consider the contribution $\propto R_V^g$. It reads

$$2\pi\alpha_{em}\left[\mathcal{H}^g_{\mu'+,\mu+}(s,t) + \mathcal{H}^g_{\mu'-,\mu-}(s,t)\right] R_V^g(t), \tag{12}$$

and is to be added to the proton helicity non-flip amplitudes $\mathcal{M}_{\mu'+,\mu+}$ in (1).

The photon–gluon amplitudes are to be calculated from the three graphs shown in Fig. 3. There are three further graphs contributing to order α_s which however reduce to the first three ones by reversing the fermion number flow. After some algebra we find for the gluon helicity non-flip amplitudes

$$\begin{aligned}
\mathcal{H}^g_{++,++} &= \frac{\alpha_s}{\pi}\left\{\frac{t^2+u^2}{2s^2}\left(\ln^2\frac{t}{u}+\pi^2\right)+\frac{t-u}{s}\ln\frac{t}{u}+1\right\},\\
\mathcal{H}^g_{-+,-+} &= \frac{\alpha_s}{\pi}\left\{\frac{s^2+t^2}{2u^2}\ln^2\frac{-t}{s}+\frac{t-s}{u}\ln\frac{-t}{s}+1\right.\\
&\quad \left.-\,\mathrm{i}\pi\left(\frac{t-s}{u}+\frac{s^2+t^2}{u^2}\ln\frac{-t}{s}\right)\right\},\\
\mathcal{H}^g_{-+,++} &= -\frac{\alpha_s}{\pi}.
\end{aligned} \tag{13}$$

Except for a different normalization these amplitudes agree with those given in [24]. In this recent paper the gluon helicity flip amplitudes can be found, too.

3 Modeling the GPDs

In order to predict wide-angle Compton scattering a model for the GPDs at large $-t$ and zero skewedness is required. In [25] (see also [4,26]) it has been shown on the basis of light-cone quantization that the GPDs possess a representation in terms of light-cone wave function overlaps. This representation allows the construction of a simple model for the GPDs by parameterizing the transverse momentum dependence of a N-particle wave function as

$$\Psi_N \propto \exp\left[-a_N^2\sum_{i=1}^{N} k_{\perp i}^2/x_i\right], \tag{14}$$

which is in line with the central assumption of the handbag approach of restricted $k_{\perp i}^2/x_i$, necessary to achieve factorization of the amplitudes into soft and hard parts. Without explicit specification of the x-dependences of the wave functions one can then calculate the $\xi = 0$ GPDs from the overlap representation if a common transverse size parameter $a = a_N$ is used. This ansatz leads to

$$\begin{aligned}
H^a(\bar{x},0;t) &= \exp\left[a^2 t\frac{1-\bar{x}}{2\bar{x}}\right] q_a(\bar{x}),\\
\widetilde{H}^a(\bar{x},0;t) &= \exp\left[a^2 t\frac{1-\bar{x}}{2\bar{x}}\right] \Delta q_a(\bar{x}),
\end{aligned} \tag{15}$$

where q_a and Δq_a are the ordinary unpolarized and polarized parton distributions for a quark of flavor a, respectively. An analogous representation holds for the gluon GPDs with the replacement of q_a and Δq_a by $\bar{x}g$ and $\bar{x}\Delta g$, respectively.

Taking the parton distributions from one of the current analyses of deep inelastic lepton–nucleon scattering, e.g. from [27], and using a value of $\simeq 1\,\mathrm{GeV}^{-1}$ for the transverse size parameter a, one obtains acceptable results for the unpolarized Compton cross section as well as for the proton and neutron electromagnetic Dirac form factors, F_1, which represent x^0-moments of H^a. The model GPDs (15) have been improved somewhat by treating the lowest three proton Fock states explicitly with specified wave functions [4,14] whose parameters are fitted to data for the electromagnetic form factors and to the parton distributions given in [27]. Due to this procedure the form factors effectively include the Sudakov factors and do practically not depend on the factorization scale. Since we are merely interested in a restricted range of momentum transfer we ignore the evolution of the GPDs as has been done in previous work [3,4,18]. As shown by Vogt [28], the evolution can be incorporated in the overlap model for the GPDs at the expense of a scale dependent transverse size parameter. Numerical results for the form factors, obtained from the improved version of the overlap model [4,18], are displayed in Fig. 4. We will employ these results in our numerical studies.

Let us now discuss the form factor R_T. The overlap representation of the underlying GPD E^a involves components of the proton wave functions where the parton helicities do not add up to the helicity of the proton. In other words, parton configurations with non-zero orbital angular momentum contribute to it. That E^a involves parton orbital angular momentum in an essential way is also reflected in Ji's angular momentum sum rule [29]. Whereas

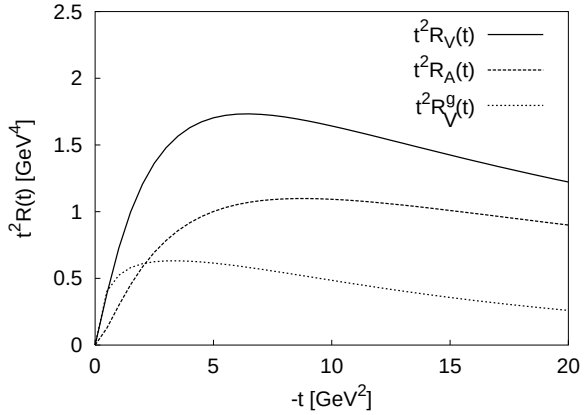

Fig. 4. The Compton form factors R_V, R_A and R_V^g, scaled by t^2, versus $-t$

R_V and F_1 represent different moments of the GPD H^a, R_T and the Pauli form factor, F_2, correspond to E^a. Since, at large $-t$, the integrals (2) for R_V and R_T as well as those for their electromagnetic counter parts, F_1 and F_2, are dominated by the region $\bar{x} \to 1$ where the valence u-quarks provide most of the contributions, there is little difference between $1/x$ and x^0-moments. This is sufficiently suggestive to assume that

$$R_T/R_V \simeq F_2/F_1. \tag{16}$$

Inspection of the SLAC data on F_2 [30] therefore leads one to the expectation $R_T/R_V \propto \Lambda^2/t$ with the consequence of parameterically suppressed ($\propto \Lambda/(-t)^{1/2}$) contributions from R_T to the Compton amplitudes (1). This has been taken as a motivation in previous LO calculations [3,4] to neglect R_T and consequently proton helicity flip. However, the recent JLab measurement of F_2 [15] seems to indicate a behavior $\propto \Lambda/(-t)^{1/2}$ for the ratio of form factors rather than Λ^2/t. Provided this behavior will be confirmed, R_T cannot be omitted in the handbag approach; it contributes to the same order in $\Lambda/(-t)^{1/2}$ as the other form factors; see (1). The results for Compton scattering presented in [3,4] have to be revised accordingly. Note that, at large $-t$, a behavior $\propto \Lambda/(-t)^{1/2}$ for the ratio of form factors appears quite natural in the overlap representation [25, 31].

In the next section we will present predictions for Compton scattering using both the scenarios R_T omitted and $R_T/R_V \propto \Lambda/(-t)^{1/2}$ for comparison. In the latter case we use a value of 0.37 for the ratio

$$\kappa = \frac{\sqrt{-t}}{2m}\frac{R_T}{R_V}, \tag{17}$$

as taken from the experimental ratio of F_2 and F_1 measured by the JLab Hall A Collaboration [15]. In general κ is a function of t.

The gluonic form factors play a minor role in our analysis since they contribute only to order α_s. Moreover, they are smaller than their quark counterparts at large $-t$ since there, as we argued above, the form factors are controlled by the region $\bar{x} \simeq 1$ where the valence u-quark dominates. R_T^g, related to E^g, as well as the gluon helicity flip form factors [17] involve parton orbital angular momentum. One may therefore anticipate that these form factors are smaller than R_V^g. R_A^g, being related to Δg, is expected to be very small, too [18]. Thus, only the largest of the gluonic form factors, R_V^g, is taken into account by us; the other ones are neglected. Numerical results for R_V^g are taken from [18] and shown in Fig. 4.

4 Observables for Compton scattering off protons

The derivation of the Compton amplitudes within the handbag approach naturally requires the use of the light-cone helicity basis. However, for comparison with experimental and other theoretical results the use of the ordinary photon–proton c.m.s. helicity basis is more convenient. The c.m.s. helicity amplitudes $\Phi_{\mu'\nu',\mu\nu}$ (we keep the notation of the helicity labels) are obtained from the light-cone helicity amplitudes (1), defined in the symmetric frame, by the following transform [17]

$$\Phi_{\mu'\nu',\mu\nu} = \mathcal{M}_{\mu'\nu',\mu\nu} + \beta/2\left[(-1)^{1/2-\nu'}\mathcal{M}_{\mu'-\nu',\mu\nu} + (-1)^{1/2+\nu}\mathcal{M}_{\mu'\nu',\mu-\nu}\right] + \mathcal{O}(\Lambda^2/t), \tag{18}$$

where

$$\beta = \frac{2m}{\sqrt{s}}\frac{\sqrt{-t}}{\sqrt{s}+\sqrt{-u}}. \tag{19}$$

For convenience we will use below a more generic notation for the six independent helicity amplitudes [32]

$$\begin{aligned} &\Phi_1 = \Phi_{++++}, \quad \Phi_3 = \Phi_{-+++}, \quad \Phi_5 = \Phi_{+-+-}, \\ &\Phi_2 = \Phi_{--++}, \quad \Phi_4 = \Phi_{+-++}, \quad \Phi_6 = \Phi_{-++-}. \end{aligned} \tag{20}$$

Inspection of (18) and (1) reveals that

$$\Phi_2 = -\Phi_6 + \mathcal{O}(\Lambda^2/t), \tag{21}$$

within the handbag approach. The amplitudes Φ_2, Φ_3 and Φ_6 are of order α_s.

In our numerical studies we choose $s/2$ as the scale of α_s which is the typical virtuality one encounters in the Feynman graphs shown in Figs. 2 and 3, and evaluate α_s from the two-loop expression for $n_f = 4$ flavors and $\Lambda^{(4)}_{\overline{\rm MS}} = 305\,{\rm MeV}$ [33]. We emphasize that our predictions, termed scenario A in the following, include corrections of order α_s and β ($\propto \Lambda/(-t)^{1/2}$) as well as contributions from R_T (with $\kappa = 0.37$). Terms of order α_s^2 and β^2 are neglected throughout. Thus, for instance, a square of a helicity amplitude is evaluated as

$$|\mathcal{H}|^2 = |\mathcal{H}^{\rm LO}|^2 + 2\mathcal{H}^{\rm LO}{\rm Re}\mathcal{H}^{\rm NLO}. \tag{22}$$

For comparison we also show the results given in [4] where only the LO subprocess amplitudes are taken into account

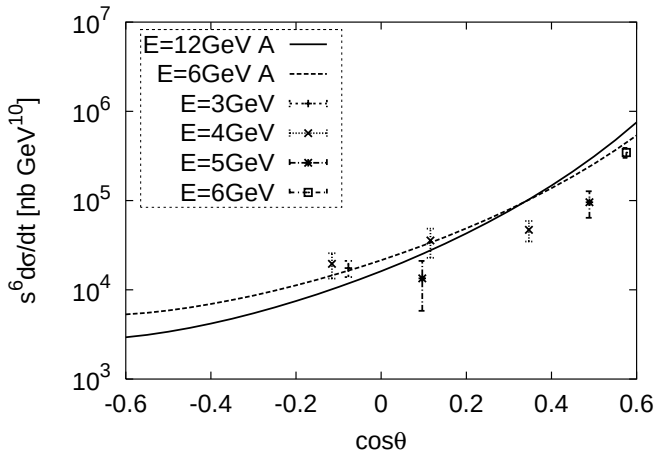

Fig. 5. Predictions from scenario A for the Compton cross section, scaled by s^6, versus $\cos\theta$ for various photon energies, E, in the laboratory frame. θ is the c.m.s. scattering angle. Data taken from [12]; they are only shown for $-t, -u \geq 2.5\,\mathrm{GeV}^2$ as a minimum condition for our approximations to be applicable

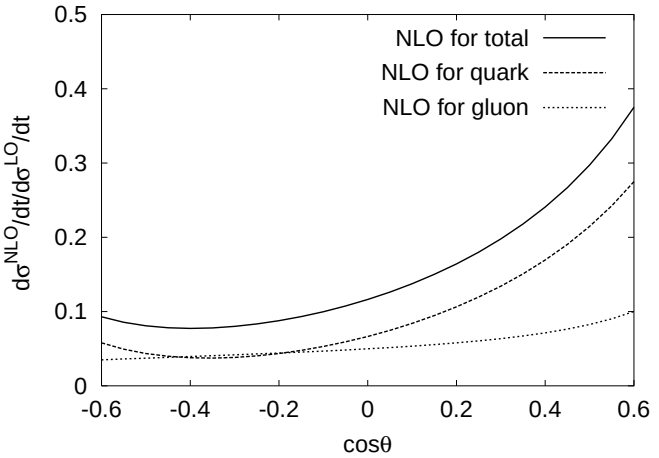

Fig. 6. Comparison between the NLO and LO results for the Compton cross section (contribution from R_T not included) at a photon laboratory energy of 6 GeV

and R_T as well as the order $\Lambda/(-t)^{1/2}$ corrections are omitted (scenario B).

The simplest but most important observable is the unpolarized cross section. In terms of the c.m.s. helicity amplitudes and within the handbag approach it reads

$$\begin{aligned}\frac{\mathrm{d}\sigma}{\mathrm{d}t} &= \frac{1}{32\pi(s-m^2)^2}\\ &\times \left[|\Phi_1|^2+|\Phi_2|^2+2|\Phi_3|^2+2|\Phi_4|^2+|\Phi_5|^2+|\Phi_6|^2\right]\\ &= \frac{\pi\alpha_{\mathrm{em}}^2}{4(s-m^2)^2}\Big\{R_V^2\left[1+\kappa^2\right]|\mathcal{H}_{++++}+\mathcal{H}_{+-+-}|^2\\ &+ R_A^2\,|\mathcal{H}_{++++}-\mathcal{H}_{+-+-}|^2+2(\mathcal{H}^{\mathrm{LO}}_{++++}+\mathcal{H}^{\mathrm{LO}}_{+-+-})\\ &\times \mathrm{Re}(\mathcal{H}^{g}_{++++}+\mathcal{H}^{g}_{+-+-})R_V R_V^g\Big\}, \qquad (23)\end{aligned}$$

where we keep the proton mass in the phase space factor. In Fig. 5 we compare our scenario A results for the Compton cross section, scaled by s^6, with experiment [12]. This scaling accounts for most of the energy dependence in the kinematical range of interest. As can be seen from Fig. 4, the form factors behave as $1/t^2$ in the momentum transfer range from about 5 to 15 GeV^2 and, consequently, the Compton cross section exhibits approximate dimensional counting rule behavior ($\propto s^{-6}$) at fixed scattering angle in a limited range of energy. With increasing $-t$ the form factors gradually turn into a $\propto t^{-4}$ behavior. In that region of t, likely well above 100 GeV^2 as is argued in [4], the perturbative contribution to Compton scattering will take the lead. For our form factor model the contribution from R_T results in a constant factor of 1.13 multiplying R_V^2 while that from R_A is very small in the forward hemisphere and grows to about 17% for $\cos\theta \simeq -0.6$. This comes about because $|\mathcal{H}_{++++}+\mathcal{H}_{+-+-}|^2 \gg |\mathcal{H}_{++++}-\mathcal{H}_{+-+-}|^2$ in the wide-angle region and because, according to the overlap model, $R_V > R_A$. In order to demonstrate the importance of the NLO corrections we display ratios of the NLO corrections for quarks and gluons and the LO result in Fig. 6. As can be seen from this figure the gluonic contribution amounts to less than 10% in the entire $\cos\theta$ range of interest. The NLO corrections from quarks are small in the backward hemisphere while the grow up to about 30% for $\cos\theta \to 1$. This happens because s and $-t$ differ greatly for $\cos\theta \to 0.6$ and, hence, some of the logs in (9) become large. $\cos\theta \simeq 0.6$ ($-t/s \simeq 0.2$) is the border line for the applicability of the handbag approach beyond which $-t$ can hardly be regarded as being of order s.

Given the quality of the data, and the small energies and low values of $-t$ and $-u$ at which they are available, the predictions following from the handbag approach are in fair agreement with experiment. Better data are clearly needed for a severe test of the handbag approach and its confrontation with other approaches. Cross sections of comparable magnitude have been obtained within a diquark model [34]. This model is a variant of the perturbative approach in which diquarks are considered as quasi-elementary constituents of the proton [35]. In the leading-twist perturbative approach, on the other hand, it seems difficult to account for the Compton data even if strongly asymmetric distribution amplitudes are used [11]. For more symmetric ones, like the asymptotic one or the one proposed in [14] the perturbative predictions are way below experiment [11].

Before we turn to the discussion of spin-dependent observables a remark concerning the definition of the proton polarization states is in order. We use the convention advocated by Bourrely, Leader and Soffer [36] and define the rotation of a vector through an azimuthal angle φ and a polar angle θ by the matrix $R(\varphi,\theta,0)$. We consider three different polarization states of the proton – L, S and N – defined as spin eigenstates of $\boldsymbol{A}\cdot\boldsymbol{\sigma}$ where $\boldsymbol{\sigma}$ is the vector formed of the Pauli matrices and $\boldsymbol{A}$ any of the unit vectors

$$\boldsymbol{L}^{(\prime)} = \frac{\boldsymbol{p}^{(\prime)}}{|\boldsymbol{p}^{(\prime)}|}, \quad \boldsymbol{N} = \boldsymbol{L}\times\boldsymbol{L}', \quad \boldsymbol{S}^{(\prime)} = \boldsymbol{N}\times\boldsymbol{L}^{(\prime)}. \qquad (24)$$

$\boldsymbol{p}$ and $\boldsymbol{p}'$ denote the three-momenta of the incoming and outgoing protons, respectively. For Compton scattering a

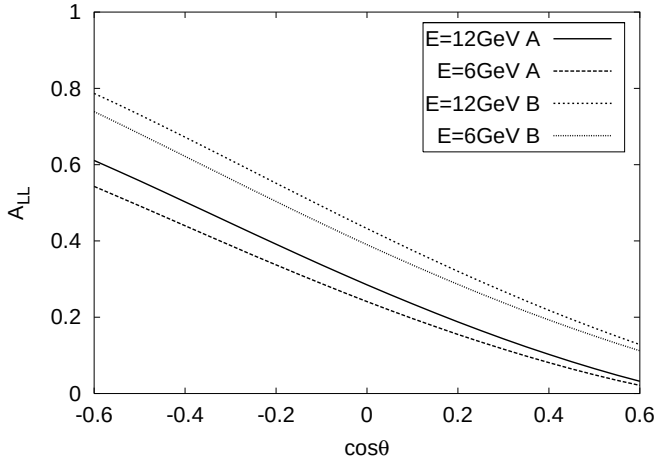

Fig. 7. Predictions for the initial state helicity correlation $A_{\rm LL}$ from scenario A and B at photon laboratory energies of 6 GeV and 12 GeV

number of polarization observables have been introduced in order to probe theoretical ideas [32], many more can be defined in principle. Obviously, only a few of them can be discussed here.

One set of polarization observables are the two-spin correlations of which the helicity (L-type) correlations are of particular interest. The one of the photon and the proton in the initial state is defined by

$$\begin{aligned} A_{LL}\frac{{\rm d}\sigma}{{\rm d}t} &= \frac{1}{2}\left[\frac{{\rm d}\sigma(++)}{{\rm d}t} - \frac{{\rm d}\sigma(+-)}{{\rm d}t}\right] \\ &= \frac{1}{32\pi(s-m^2)^2}\left[|\Phi_1|^2 + |\Phi_2|^2 - |\Phi_5|^2 - |\Phi_6|^2\right] \\ &= \frac{\pi\alpha_{\rm em}^2}{2(s-m^2)^2}R_A\Big\{R_V[1-\beta\kappa] \\ &\quad\times[|\mathcal{H}_{++++}|^2 - |\mathcal{H}_{+-+-}|^2] \\ &\quad + R_V^g(\mathcal{H}^{\rm LO}_{++++} - \mathcal{H}^{\rm LO}_{+-+-}) \\ &\quad\times{\rm Re}(\mathcal{H}^g_{++++} + \mathcal{H}^g_{+-+-})\Big\}. \end{aligned} \tag{25}$$

Using the model form factors discussed in Sect. 3, we evaluate the initial state helicity correlation A_{LL} for scenario A and compare it in Fig. 7 to that obtained from scenario B [4]. The $\cos\theta$ dependence of A_{LL} approximately reflects that of the corresponding helicity correlation for the photon–parton subprocess, $(s^2-u^2)/(s^2+u^2)$, its size being however diluted by the form factors. We observe from Fig. 7 that the inclusion of R_T and the NLO corrections reduce the values of A_{LL} by about 0.1 to 0.2 as compared to the results from scenario B. The results from the handbag approach are opposite in sign to the diquark model predictions [34]. In the leading-twist perturbative approach, the results for A_{LL} are also markedly different from our ones [11]. They are very sensitive to the proton distribution amplitudes used in the evaluation.

The analogous correlation between the helicities of the incoming photon and the outgoing proton is defined by

$$\begin{aligned} K_{LL}\frac{{\rm d}\sigma}{{\rm d}t} &= \frac{{\rm d}\sigma(++)}{{\rm d}t} - \frac{{\rm d}\sigma(+-)}{{\rm d}t} \\ &= \frac{1}{32\pi(s-m^2)^2}\left[|\Phi_1|^2 - |\Phi_2|^2 - |\Phi_5|^2 + |\Phi_6|^2\right]. \end{aligned} \tag{26}$$

Since $\Phi_2 = -\Phi_6$ in the handbag approach, see (21), we obtain

$$K_{LL} = A_{LL}. \tag{27}$$

The helicity transfer from the incoming to the outgoing photon reads

$$\begin{aligned} D_{LL}\frac{{\rm d}\sigma}{{\rm d}t} &= \frac{{\rm d}\sigma(++)}{{\rm d}t} - \frac{{\rm d}\sigma(+-)}{{\rm d}t} \\ &= \frac{1}{32\pi(s-m^2)^2}\Big[|\Phi_1|^2 - |\Phi_2|^2 - 2|\Phi_3|^2 + 2|\Phi_4|^2 \\ &\quad + |\Phi_5|^2 - |\Phi_6|^2\Big]. \end{aligned} \tag{28}$$

Although the photon helicity is not strictly conserved to NLO, the helicity transfer is

$$D_{LL} = 1 + \mathcal{O}(\alpha_{\rm s}^2), \tag{29}$$

as is evident from a comparison of (23) and (28).

One may also consider sideway proton spin directions; see (24). The correlation between the helicity of the incoming photon and the sideway (S-type) polarization of the incoming proton, parallel ($\rightarrow$) or antiparallel ($\leftarrow$) to the S-direction reads

$$\begin{aligned} A_{LS}\frac{{\rm d}\sigma}{{\rm d}t} &= \frac{1}{2}\left[\frac{{\rm d}\sigma(+\rightarrow)}{{\rm d}t} - \frac{{\rm d}\sigma(-\rightarrow)}{{\rm d}t}\right] \\ &= \frac{1}{16\pi(s-m^2)^2}{\rm Re}\left[(\Phi_1-\Phi_5)\Phi_4^* - (\Phi_2+\Phi_6)\Phi_3^*\right] \\ &= -\frac{\pi\alpha_{\rm em}^2}{2(s-m^2)^2}R_A \\ &\quad\times\left\{\frac{\sqrt{-t}}{2m}R_T[1+\beta\kappa^{-1}][|\mathcal{H}_{++++}|^2 - |\mathcal{H}_{+-+-}|^2]\right. \\ &\quad + \beta R_V^g(\mathcal{H}^{\rm LO}_{++++} - \mathcal{H}^{\rm LO}_{+-+-}) \\ &\quad\left.\times\,{\rm Re}(\mathcal{H}^g_{++++} + \mathcal{H}^g_{+-+-})\right\}. \end{aligned} \tag{30}$$

Predictions from scenario A are shown in Fig. 8, those obtained from scenario B are zero. A_{LS} turns out to be rather independent of the photon energies. It is important to note that A_{LS} is an observable that is very sensitive to the form factor R_T. The corrections from the term $\beta\kappa^{-1}$ are, however, substantial, in particular for the energies available at JLab; they cannot be ignored. This, after all, is the reason why, in contrast to [3,4], we keep these terms. Neither in the diquark model [34] nor in the leading-twist perturbative approach [11] the observable A_{LS} has been discussed.

The correlation between the helicity of the incoming photon and the sideway polarization of the outgoing proton is defined as

$$K_{LS}\frac{{\rm d}\sigma}{{\rm d}t} = \frac{{\rm d}\sigma(+\rightarrow)}{{\rm d}t} - \frac{{\rm d}\sigma(-\rightarrow)}{{\rm d}t}$$

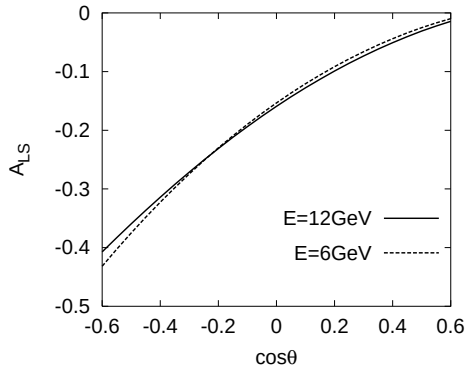

Fig. 8. The correlation A_{LS} at photon laboratory energies of 6 GeV and 12 GeV

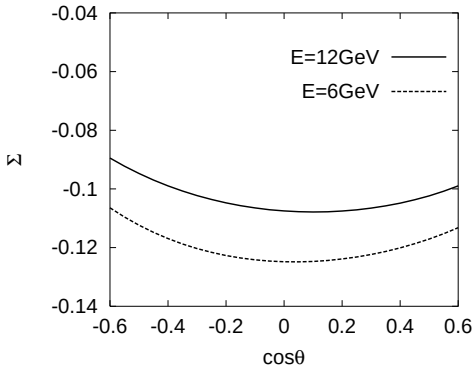

Fig. 9. The incoming photon asymmetry Σ at photon laboratory energies of 6 GeV and 12 GeV

$$= -\frac{1}{16\pi(s-m^2)^2} \times \mathrm{Re}\left[(\Phi_1-\Phi_5)\Phi_4^* + (\Phi_2+\Phi_6)\Phi_3^*\right]. \quad (31)$$

Because of $\Phi_2 = -\Phi_6$ it follows that

$$K_{LS} = -A_{LS}. \quad (32)$$

Correlations between the helicity of the incoming photon and the transverse (N-type) polarization of either the incoming or the outgoing proton are zero due to parity invariance

$$K_{LN} = A_{LN} = 0. \quad (33)$$

A single-spin observable for Compton scattering is the incoming photon asymmetry Σ which is defined as

$$\begin{aligned}\Sigma\frac{\mathrm{d}\sigma}{\mathrm{d}t} &= \frac{1}{2}\left[\frac{\mathrm{d}\sigma_\perp}{\mathrm{d}t} - \frac{\mathrm{d}\sigma_\parallel}{\mathrm{d}t}\right] \\ &= \frac{1}{16\pi(s-m^2)^2}\mathrm{Re}\left[(\Phi_1+\Phi_5)\Phi_3^* + (\Phi_2-\Phi_6)\Phi_4^*\right] \\ &= \frac{\alpha_\mathrm{s}\alpha_\mathrm{em}^2}{(s-m^2)^2}\frac{(s-u)^2}{us} \\ &\quad\times\left[C_F R_V^2(1+\kappa^2) + 2\frac{\sqrt{-us}}{s-u}R_V R_V^g\right], \end{aligned} \quad (34)$$

where $\perp$ and $\parallel$ refer to linear photon polarization normal to and in the scattering plane, respectively. Obviously, Σ is zero to LO since there is no photon helicity flip. The predictions obtained from scenario A are shown in Fig. 9. Σ is negative and small in absolute value. Approximately, i.e. if the terms $\propto R_A$ and $\propto R_V^g$ are neglected in (23) and (34), it is given by

$$\Sigma \simeq -\alpha_\mathrm{s} C_F/\pi. \quad (35)$$

Hence, the incoming photon asymmetry is nearly independent of the Compton form factors. In the diquark model [34] Σ is negative too but smaller in absolute value. The leading-twist approach [11], on the other hand, provides rather large positive values for Σ.

Last but not least we want to comment on the (N-type) polarization or, as occasionally termed, the single-spin asymmetry of the incoming proton, that of the outgoing one is analogous. The polarization of the incoming proton is defined by

$$\begin{aligned} P\frac{\mathrm{d}\sigma}{\mathrm{d}t} &= \frac{1}{2}\left[\frac{\mathrm{d}\sigma(\uparrow)}{\mathrm{d}t} - \frac{\mathrm{d}\sigma(\downarrow)}{\mathrm{d}t}\right] \\ &= \frac{1}{16\pi(s-m^2)^2}\mathrm{Im}\left[(\Phi_1+\Phi_5)\Phi_4^* - (\Phi_2-\Phi_6)\Phi_3^*\right], \end{aligned} \quad (36)$$

where $\uparrow$ and $\downarrow$ denote the proton polarization parallel and antiparallel to the N-direction, respectively. The calculation of that polarization is a notoriously difficult task within QCD. Therefore, many experimentally observed polarization effects, as for instance the polarization in proton–proton elastic scattering at large momentum transfer [37], remained unexplained. As is well known a non-zero polarization requires proton helicity flip and phase differences between the various helicity amplitudes. Both the necessary ingredients are provided by the handbag approach, helicity flips from R_T and phases from the NLO corrections and we approximately obtain

$$P \simeq -\frac{\sqrt{-t}}{2m}\frac{R_T R_V^g}{R_V^2}\frac{\sqrt{-us}}{s-u}\mathrm{Im}\big(\mathcal{H}^g_{++++} + \mathcal{H}^g_{+-+-}\big). \quad (37)$$

The polarization is of order α_s and proportional to the gluonic contribution. Numerically it is very small, less than 3% for our model form factors. The predictions for P are to be taken with a grain of salt. The neglect of gluon helicity flip as well as α_s^2 and Λ^2/t terms may lead to substantial corrections. Thus, in a conservative estimate, we can only say that an experimentally observed polarization larger in absolute value than, say, 0.1–0.2 near $\theta = 90^\circ$ would be difficult to understand in the handbag approach.

5 Measuring the Compton form factors

In the preceding section we presented predicitions for various observables of wide-angle Compton scattering within the handbag approach, using a model for the form factors that is based on light-cone wave function overlaps [4, 25]. On the other hand, a model-independent test of the handbag approach is provided by a measurement of the Compton form factors which can be performed through an analysis of the data for a set of observables to be at our disposal for several values of s and t. The crucial question is whether or not the experimentally determined form

Table 1. The discrepancies between the approximations (38) and the full results from scenario A in percent of the full results at a photon laboratory energy of 6 GeV

$\cos\theta$	$\Delta(\mathrm{d}\sigma/\mathrm{d}t)$ [%]	$\Delta(K_{LL})$ [%]	$\Delta(K_{LS}/K_{LL})$ [%]
0.6	-6.2	15.0	1.4
0	-5.6	2.4	2.2
-0.6	-14.8	-11.2	14.6

factors are independent of s within the experimental and theoretical uncertainties.

At JLab the E99-114 collaboration plans to measure along with the differential cross section the two-spin correlations K_{LL} and K_{LS} [38]. Provided the quality of this data will be sufficiently good one may isolate the three form factors $R_V(t)$, $R_A(t)$ and $R_T(t)$ (or $\kappa(t)$) from it. As a first step towards a model-independent analysis, one may neglect the gluonic contributions everywhere and the term $\propto R_A$ in the cross section which, as we discussed above, is small. To the extent that these simplifications are justified, one finds

$$\begin{aligned}
\frac{\mathrm{d}\sigma}{\mathrm{d}t} &\simeq \frac{\pi\alpha_{\mathrm{em}}^2}{4(s-m^2)^2} R_V^2(t)[1+\kappa^2(t)]\left|\mathcal{H}_{++++}+\mathcal{H}_{+-+-}\right|^2,\\
K_{LL} &\simeq 2\frac{R_A(t)}{R_V(t)}\frac{1-\beta\kappa(t)}{1+\kappa^2(t)}\frac{\left|\mathcal{H}_{++++}\right|^2-\left|\mathcal{H}_{+-+-}\right|^2}{\left|\mathcal{H}_{++++}+\mathcal{H}_{+-+-}\right|^2},\\
\frac{K_{LS}}{K_{LL}} &\simeq \kappa(t)\frac{1+\beta\kappa^{-1}(t)}{1-\beta\kappa(t)}. \qquad (38)
\end{aligned}$$

The cross section is essentially controlled by the form factor R_V with, probably, only a small correction from κ. K_{LL} measures the ratio R_A/R_V with, however, substantial corrections from κ. The ratio K_{LS}/K_{LL} determines the Compton analogue R_T/R_V ($\propto\kappa$) to the ratio of the electromagnetic form factors F_2 and F_1. For large energies and scattering angles near 90°, the β terms are negligibly small and the analysis is markedly simplified. In Table 1 we present an assessment of the quality of the approximations (38). The discrepancies between (38) and the full results from scenario A do not exceed 15% at a photon energy of 6 GeV. The use of the LO amplitudes in (38) instead of the NLO ones enlarges the discrepancies, in particular in the forward hemisphere; see Fig. 6. The form factors measured through (38) may be improved iteratively.

6 Summary

As a complement to [4] we have calculated the NLO QCD corrections to the subprocess amplitudes and include the form factor R_T, related to the GPD E, in the analysis of wide-angle Compton scattering off protons. We have also considered the difference between the light-cone helicity basis in which the handbag graph is calculated, and the usual c.m.s. helicity one. Predictions for various Compton observables are given and compared to the leading contribution discussed in [4]. It turns out that these corrections are non-negligible in general although not unreasonably large. The NLO corrections and those due to the change of the helicity basis decrease with increasing energy while those due to the form factor R_T keep their size provided κ is independent of t. We stress that there are uncontrolled corrections of order Λ^2/t in the handbag approach. For energies as low as, say, 3 GeV these corrections may be substantial. Our study may be of importance for severe tests of the handbag approach with future high-quality data for wide-angle Compton scattering which might be obtained at Spring-8, JLab or an ELFE-type accelerator.

Acknowledgements. One of the authors (H.W.H.) would like to thank the Monbusho's Grand-in-Aid for the JSPS postdoctoral fellow for financial support. P.K. wishes to acknowledge discussions with Markus Diehl, Rainer Jakob and Dieter Müller.

References

1. A.V. Radyushkin, Phys. Rev. D **56**, 5524 (1997) [hep-ph/9704207]
2. X. Ji, J. Osborne, Phys. Rev. D **58**, 094018 (1998) [hep-ph/9801260]; J.C. Collins, A. Freund, Phys. Rev. D **59**, 074009 (1999) [hep-ph/9801262]
3. A.V. Radyushkin, Phys. Rev. D **58**, 114008 (1998) [hep-ph/9803316]
4. M. Diehl, T. Feldmann, R. Jakob, P. Kroll, Eur. Phys. J. C **8**, 409 (1999) [hep-ph/9811253]; Phys. Lett. B **460**, 204 (1999) [hep-ph/9903268]
5. X. Ji, Phys. Rev. D **55**, 7114 (1997) [hep-ph/9609381]
6. D. Müller, D. Robaschik, B. Geyer, F.M. Dittes, J. Hořejši, Fortsch. Phys. **42**, 101 (1994) [hep-ph/9812448]
7. J.D. Bjorken, E.A. Paschos, Phys. Rev. **185**, 1975 (1969)
8. D.M. Scott, Phys. Rev. D **10**, 3117 (1974)
9. G.P. Lepage, S.J. Brodsky, Phys. Rev. D **22**, 2157 (1980)
10. G.R. Farrar, H. Zhang, Phys. Rev. D **41**, 3348 (1990) [Erratum ibid. D 42 (1990) 3348]; A. Kronfeld, B. Nižić, Phys. Rev. D **44**, 3445 (1991); Erratum Phys. Rev. D **46**, 2272 (1992); M. Vanderhaeghen, P.A.M. Guichon, J. Van de Wiele, Nucl. Phys. A **622**, 144c (1997)
11. T.C. Brooks, L. Dixon, Phys. Rev. D **62**, 114021 (2000) [hep-ph/0004143] and private communication
12. M.A. Shupe et al., Phys. Rev. D **19**, 1921 (1979)
13. A.V. Radyushkin, Nucl. Phys. A **532**, 141c (1991); N. Isgur, C.H. Llewellyn Smith, Nucl. Phys. B **317**, 526 (1989); R. Jakob, P. Kroll, M. Raulfs, J. Phys. G **22**, 45 (1996) [hep-ph/9410304]
14. J. Bolz, P. Kroll, Z. Phys. A **356**, 327 (1996) [hep-ph/9603289]
15. M.K. Jones et al. [Jefferson Lab Hall A Collaboration], Phys. Rev. Lett. **84**, 1398 (2000) [nucl-ex/9910005]
16. J.B. Kogut, D.E. Soper, Phys. Rev. D **1**, 2901 (1970)
17. M. Diehl, Eur. Phys. J. C **19**, 485 (2001) [hep-ph/0101335]
18. H.W. Huang, P. Kroll, Eur. Phys. J. C **17**, 423 (2000) [hep-ph/0005318]
19. J.C. Collins, Sudakov Form-Factors, in Perturbative Quantum Chromodynamics, edited by A.H. Mueller, pp. 573–614 and references therein
20. I.V. Musatov, A.V. Radyushkin, Phys. Rev. D **56**, 2713 (1997) [hep-ph/9702443]

21. L.M. Brown, R.P. Feynman, Phys. Rev. **85**, 231 (1952)
22. A.V. Belitsky, D. Müller, Phys. Lett. B **417**, 129 (1998) [hep-ph/9709379]; L. Mankiewicz, G. Piller, E. Stein, M. Vanttinen, T. Weigl, Phys. Lett. B **425**, 186 (1998) [hep-ph/9712251]
23. D. Müller, private communication
24. Z. Bern, A. De Freitas, L.J. Dixon, JHEP **0109**, 037 (2001) [hep-ph/0109078]
25. M. Diehl, T. Feldmann, R. Jakob, P. Kroll, Nucl. Phys. B **596**, 33 (2001) [Erratum ibid. B **605**, 647 (2001)] [hep-ph/0009255]
26. S.J. Brodsky, M. Diehl, D.S. Hwang, Nucl. Phys. B **596**, 99 (2001) [hep-ph/0009254]
27. M. Glück, E. Reya, A. Vogt, Z. Phys. C **67**, 433 (1995); Eur. Phys. J. C **5**, 461 (1998) [hep-ph/9806404]; M. Glück, E. Reya, M. Stratmann, W. Vogelsang, Phys. Rev. D **53**, 4775 (1996) [hep-ph/9508347]
28. C. Vogt, Phys. Rev. D **63**, 034013 (2001) [hep-ph/0007277]
29. X. Ji, J. Phys. G **24**, 1181 (1998) [hep-ph/9807358]
30. L. Andivahis et al., Phys. Rev. D **50**, 5491 (1994)
31. J.P. Ralston, P. Jain, R. Buniy, contribution to the Conference on Intersections of Particle and Nuclear Physics, Quebec (2000); P. Kroll, contribution to the 9th International Workshop on Deep Inelastic Scattering, Bologna (2001), hep-ph/0106191
32. H. Rollnik, P. Stichel, in E. Paul et al., Elementary Particle Physics, Springer Tracts Vol.79, Berlin 1976
33. C. Caso et al. [Particle Data Group Collaboration], Eur. Phys. J. C **3**, 1 (1998)
34. P. Kroll, M. Schürmann, W. Schweiger, Int. J. Mod. Phys. A **6**, 4107 (1991)
35. M. Anselmino, P. Kroll, B. Pire, Z. Phys. C **36**, 89 (1987)
36. C. Bourrely, J. Soffer, E. Leader, Phys. Rept. **59**, 95 (1980)
37. P.R. Cameron et al., Phys. Rev. D **32**, 3070 (1985)
38. A.M. Nathan, hep-ph/9908522